Chapter 5

Charge Separation is Virtually Irreversible in Intact Photosystem II Cores

C.D. van der Weij – de Wit, I.H.M. van Stokkum, E. Schlodder, R. van Grondelle, J.P. Dekker, to be submitted

X-ray structures of the Photosystem II (PSII) core revealed relatively large inter-pigment distances between the CP43 and CP47 antenna complexes and the reaction center (RC) with respect to the inter-pigment distances in a single unit (Loll et al. 2005). This finding questioned the possibility of fast energy equilibration among the antenna and the RC, which had been assumed to explain measured PSII fluorescence kinetics (Van Grondelle 1985, Schatz et al. 1988). In this study, we present time-resolved fluorescence measurements on intact PSII cores at room temperature. Kinetic modeling of the data reveals that the kinetics are best described by fast primary charge separation at a time scale of 1.5 ps and slow energy transfer from the antenna into the RC, which results in an energy equilibration time between the antenna and the RC of about 44 ps. Primary radical pair formation was found to be a virtually irreversible process, which agrees well with predictions from the X-ray structure (Broess et al. 2006). Energy equilibration in the CP43 and CP47 complexes is shown to occur at a time scale of 7.7 ps. The time-resolved measurements were repeated at 77 K and, upon kinetic modeling, reveal similar energy transfer time scales in the antenna units and among the antenna and the RC as at room temperature, respectively 7 and 37 ps. We conclude that the energy transfer from the CP43/CP47 antenna to the RC can not be neglected in the total charge separation kinetics in intact cores.

Introduction

Photosystem II (PSII) is a large supra-molecular pigment-protein complex which is embedded in the thylakoid membrane of plants, cyanobacteria and algae. In oxygenic photosynthesis, PSII catalyzes watersplitting to create a proton gradient across the membrane and to form oxygen, using light-energy as the driving force. PSII consists of a core complex surrounded by several antenna pigment-protein complexes, which efficiently collect light and transfer the energy into the core (Van Grondelle et al. 1994). The X-ray structure of the cyanobacterial PSII core has been resolved up to 3.0 Å resolution (Zouni et al. 2001, Ferreira et al. 2004, Loll et al. 2005). Natively, PSII cores are organized into dimers in the stacked parts of the membrane (Dekker and Boekema 2005). The PSII core consists of at least 17 subunits (Zouni et al. 2001, Ferreira et al. 2004, Loll et al. 2005). Proteins PsbB and PsbC bind respectively 16 and 13 Chl *a* and are known as the CP47 and CP43 core antenna complexes, which flank both sides of the PSII reaction centre (RC), comprised respectively by PsbA and PsbD. CP43 and CP47 take care of the efficient transfer of light-energy into the RC. In the RC, light-energy is used for charge separation (CS), resulting in the watersplitting. PsbA and PsbD provide the ligands for the cofactors present in the electron transfer chain, where PsbA constitutes the active branch and PsbD the inactive branch (Diner and Rappaport 2002). The cofacters are 6 Chl *a*, 2 Pheo *a*, 2 plastoquinones (Q_A, Q_B), 2 redox-active tyrosines (Y_Z, Y_D), a non-heme iron and the manganese cluster. An electron is induced to transfer from the primary donor Chl_{D1} to Pheo (Groot et al. 2005, Holzwarth et al. 2006), which passes it through to the quinone acceptor Q_A (see Dekker and Van Grondelle 2000, Diner and Rappaport 2001, Nelson and Yocum 2006, for reviews on charge separation). P_{680} is a central Chl *a* dimer which transfers an electron to Chl_{D1} and subsequently withdraws an electron from the manganese cluster, which is mediated by Y_Z. Upon the uptake of four photons resulting in CS, Q_A doubly reduces two mobile Q_B molecules, whereas at the manganese cluster the four positive charges possess enough strength to oxidize two water molecules. Four hydrogen ions associate with the two doubly reduced Q_B molecules. The H_2Q_B complexes are released into the plastoquinone pool and are replaced by a Q_B from the pool such that the sequence of light-driven electron transfers can be repeated.

Early time-resolved studies on PSII cores revealed the excitation energy trapping to be multiphasic (Schatz et al. 1987). The Exciton Radical Pair Equilibrium (ERPE) model was developed to describe this behavior (Van

Grondelle 1985, Schatz et al. 1988). In this model, the RC forms a shallow trap from which reversible CS is possible. The main assumption of the model is the occurrence of fast energy equilibration over the core antenna and RC prior to CS. As a result, the model describes trap-limited CS in the PSII cores. The trapping time scales were found to depend on the presence of antenna units as well as the redox-state of the primary quinone acceptor Q_A (Schatz et al. 1988, Van Mieghem et al. 1992). Nowadays, the time scale of the energy equilibration over the complex is under debate, since from the X-ray structure (Zouni et al. 2001, Ferreira et al. 2004, Loll et al. 2005) the inter-pigment distance between antenna and RC (~20 Å) appears rather large with respect to the inter-pigment distance within a singe unit (5-10 Å), which may limit energy transfer to the RC (Vassil'ev et al. 2001 and 2002, Broess et al. 2006).

Recently, Miloslavina and co-workers (2006) measured the fluorescence kinetics of intact PSII cores with open RCs, using the single photon counting technique. They were the first ones to resolve emission decay components on the short time scale, namely 2 and 9 ps. The 2 ps decay was assigned to fast excitation energy transfer from the antenna into the RC and the 9 ps component was split into 7 and 10 ps contributions by respectively primary radical pair (RP1) formation and energy equilibration between CP43 to CP47 through the RC. The commonly known ~40 ps main excitation energy trapping component of the PSII core was assigned to second radical pair (RP2) (P^+Pheo^-) formation. In their modeling, Miloslavina and co-workers (2006) thus assume the energy transfer among the core antenna and the RC to be unreasonably fast with respect to the predictions from the molecular structure as discussed by (Vasil'ev et al. 2001 and 2002, De Weerd et al. 2002a, Broess et al. 2006). Pawlowicz and co-workers (2007) show in their recent femtosecond mid-infrared spectroscopic study of the PSII core that slow energy transfer from the CP43 and CP47 antennae to the RC is the physical origin of the 40 ps main excitation energy trapping component in PSII cores.

The lack of consensus on the interpretation of time-resolved studies of the PSII core calls for new measurements and analysis. In this study we aim to enlighten the role of excitation energy transfer from the antenna into the RC in the total CS process for PSII cores with open, functional reaction centra. To this end, room temperature time-resolved fluorescence was measured of PSII cores from *Thermosynechococcus elongatus* with Q_A oxidized, with a streak camera setup, which offers the possibility to simultaneously measure the fluorescence decay over a ~300 nm wavelength range with far better time-resolution (5 ps) than the single photon counting detection technique used by Miloslavina and co-workers (2006)

(typically > 30 ps). Then, the measurements were repeated at 77 K, which focus on the transfer of excitation energy from the core antenna to the RC.

Materials and Methods

Sample preparation

Dimeric PSII core complexes with both Q_A and Q_B present were isolated from *Thermosynechococcus elongatus* and purified as described by (Kern et al. 2005). In brief, after cell disruption and centrifugation, thylakoid membranes were solubilized with n-ß-D-dodecylmaltoside (ß-DM) and PSII was purified using a two-step anion exchange chromatography. The dimeric PSII was further purified by crystallization using PEG 2000 as precipitant. The obtained micro-crystals were redissolved in 100 mM Pipes-NaOH, 5 mM $CaCl_2$ and 0.03% ß-DM. The concentrated protein solution was frozen in liquid nitrogen and stored at 77 K. The PSII complexes are characterized by an O_2 flash yield of about 6 10^{-3} O_2/Chl per flash.

Time-resolved emission

Briefly, 400 nm, vertically polarized excitation pulses of 100-200 fs were generated using the frequency doubled output of a Ti:sapphire laser (VITESSE, Coherent St. Clara, CA) and a regenerative amplifier (REGA, Coherent). Fluorescence light was collected at right angle to the excitation light, under magic angle through an orange sharp cut off filter, using a Chromex 250IS spectrograph and a Hamamatsu C 5680 synchroscan streak camera. The streak images were recorded with a cooled, Hamamatsu C4880 CCD camera.

For the room temperature measurements, the excitation light was collimated with a 15 cm focal length lens, resulting in a focal diameter of 150 μm in the sample. The laser repetition rate was 300 kHz and the pulse energy 0.1 nJ. The sample was in a 2 mm spinning cell of 10 cm diameter, rotating at a frequency of 75 Hz. PSII cores were diluted to an optical density of 0.6 cm^{-1} at 673 nm in a buffer of 20 mM MES pH 6.5, 10 mM $CaCl_2$, 10 mM $MgCl_2$, 400 mM mannitol, 0.06% β-DM and 5 mM ferricyanide was added to keep Q_A oxidized. Under these low excitation density conditions (~1 absorbed photon per 50 dimeric cores), the experiments are expected to be free of annihilation.

For the 77 K measurements, an unfocussed excitation beam was used with a diameter of ~1 mm. The laser repetition rate was 50 kHz and the pulse energy 10 nJ. The sample was in a 1 cm polystyrene cuvette in a nitrogen cryostat (Oxford).

At 77 K, the fluorescence was detected in front-face mode. PSII cores were diluted in a buffer of 65% v/v glycerol, 20 mM MES pH 6.5, 10 mM $CaCl_2$, 10 mM $MgCl_2$, 400 mM mannitol and 0.09% β-DM to an optical density of 1.0 cm^{-1} at 673 nm.

The fluorescence was measured on time-bases of 500 and 2000 ps, with respective full-width at half-maximum (FWHM) of the overall time response of 5 and 21 ps at room temperature and 9 and 21 ps at 77 K. In the global analysis, both the instrument response and time dispersion were free parameters of the fit.

The datasets obtained with the streak camera setup, consist of two-dimensional images of fluorescence intensity as a function of both time and wavelength. Before analysis, the images are corrected for background and sensitivity of the detection system. The images are sliced up into time traces which span 4 nm. In global analysis, the time traces are fit with a sum of exponentials with different decay times. The amplitudes of these exponentials as a function of emission wavelength give the so-called decay associated spectra (DAS). In these spectra, positive amplitude represents a loss of fluorescence, whereas negative amplitude reflects a rise of fluorescence. A DAS with positive amplitude at short wavelengths and negative amplitude at higher wavelengths thus represents an energy transfer process, whereas an overall positive spectrum describes either trapping of excitations by CS or a natural fluorescence emission of the pigments (the latter occurs typically at the ns- time scale). For more details, see (Holzwarth 1996, Van Stokkum et al. 2004). In target analysis, a kinetic model consisting of several pigment pools interconnected by energy/electron transfer rate-constants is fit to the data, resulting in species associated spectra (SAS). For details, see (Holzwarth 1996, Van Stokkum et al. 2004).

Results and Discussion

Room temperature time-resolved emission

Time-resolved fluorescence was recorded at room temperature upon 400 nm excitation. The initial excitation population will thus be homogeneously distributed over the pigments of the PSII core complex. The fluorescence time traces were subjected to global analysis. The resulting DAS are shown in Figure 1. The data could be well described by 5 decay components. The first resolved DAS with a decay time of 0.7 ps shows overall negative amplitude with maximum at 681.5 nm and is assigned to the fluorescence rise due to Soret to Q_y relaxation. The second DAS is associated with a 12 ps decay time and is multiplied in Figure 1 by

a factor of two for clarity. This DAS has a positive maximum between 669 and 687 nm. The main (well-known) PSII core decay component was resolved to have a 49 ps lifetime, with emission maximum at 682 nm. The fourth DAS has only minor amplitude, a 223 ps time-constant and a maximum emission at 682 nm, which is multiplied in Figure 1 by a factor of two for clarity. Careful analysis revealed a 1.4 ns lifetime component which is estimated to trap less than 1.5% of the initial excitations, and has a noisy spectrum. Both the 49 and 223 ps decay times are values commonly found in the literature on PSII cores with Q_A oxidized (Van Mieghem et al. 1992, Vasil'ev et al. 2002, Miloslavina et al. 2006). However, in our data the fluorescence decay on the ns-timescale was nearly negligible, in contrast with other studies on PSII cores where the PSII RC was claimed to be open (Van Mieghem et al. 1992, Vasil'ev et al. 2002). Figure 2 displays a selection

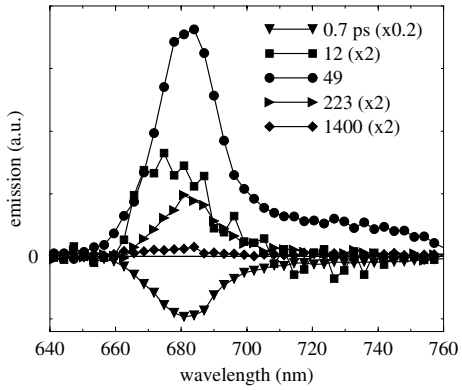

Fig 1. DAS of intact PSII cores with open RCs at room temperature upon 400 nm excitation.

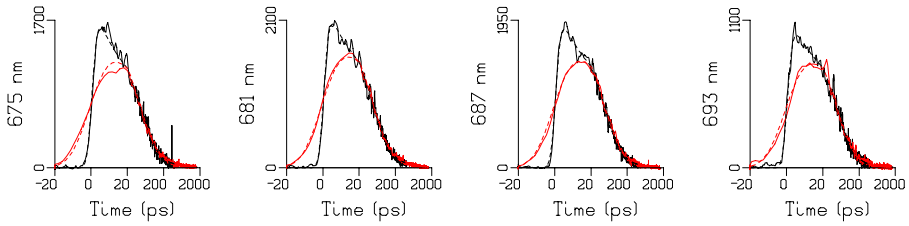

Fig 2. Fluorescence time traces (solid) and the global fit (dash) of Figure 1 on a time scale of 0.5 ns (black) and 2 ns (red), with respective timeresponses of 5 and 21 ps FWHM, for wavelengths 675, 681, 687 and 693 nm. Note that the time axis is linear from -20 to 20 ps and logarithmic thereafter.

of time traces with their fits, showing both the fit quality and the near absence of long lifetime fluorescence, since there is hardly emission left after 1 ns. It is known that it is really hard to avoid closure of a small fraction of PSII RCs, which results in the presence of ns decay components. In fact, it took us multiple efforts, varying excitation density, data acquisition time per PSII core sample, and electron acceptor concentration, before we managed to get to the right set of conditions in which >98.5% of the RCs remain open. The main problem was to tune the time it takes for a sample volume to get re-excited and the Q_A^- oxidation time by the electron acceptor, such as to avoid re-excitation of the small fraction of PSII cores with reduced Q_A. As a result, one should either have a big reservoir of PSII cores, or one can measure with really low excitation density for only a short period on a limited amount of sample (at the cost of the signal-to-noise (S/N) ratio), to be sure not to re-excite unrelaxed cores. However, in all our different efforts the ~10 ps decay with the characteristic contribution of blue 670-675 nm emission (Figure 1) was present (not shown). We emphasize that our 12 ps DAS differs significantly from the 9 ps DAS resolved by (Miloslavina et al. 2006), which has its emission maximum at 685 nm: the 12 ps DAS in Figure 1 has extra amplitude of similar size around 673 nm. The blue (673 nm) emission amplitude in the 12 ps DAS with respect to those with 49 and 223 ps decay time (682 nm maximum), demonstrates the occurrence of energy transfer from blue to more red absorbing Chls *a* on this time scale. The absence of negative amplitude at wavelengths above 673 nm in the 12 ps DAS indicates the simultaneous decay of the emission at these more red wavelengths at the same, or a faster, time scale due to trapping.

Kinetic modeling

In order to unravel the processes underlying the spectral evolution taking place on the different time scales determined in global analysis, a target analysis was performed. In target analysis, a kinetic model is established, which satisfactorily describes the fluorescence decay. The minimal model, which successfully describes the recorded room temperature PSII core kinetics, comprises 4 compartments and is shown in Figure 3 with the optimal rate-constants and free energy associated with RP1 formation. The S/N quality of the data and the small difference in spectral characteristics of CP47 and CP43 at room temperature did not allow CP43 and CP47 to be spectrally distinguished. Therefore, we considered CP43 and CP47 as a single entity, the antenna. The model takes however into account the presence of a fraction of pigments which absorb more to the blue than the other pigments in the CP43/CP47 antenna (De Weerd et al. 2002b). This

distinction is made by describing these respective pigment pools with the two compartments (bA) and (A) in the model of Figure 3, were (bA) equilibrates with (A). Then, we can describe the fluorescence kinetics well by further equilibration of the relaxed antenna (A) with the RC (RC). From the RC CS can occur – formation of (RP1) – which is reversible as shown by the back transfer, whereas from RP1 the excitation energy is irreversibly trapped by the 4.9 ns^{-1} process. In reality, electron transfer in the RC comprises three steps before Q_A becomes oxidized by ferricyanide, respectively the formation of $Chl_{D1}^{+}Pheo^{-}$, $P_{680}^{+}Pheo^{-}$, and $P_{680}^{+}Q_A^{-}$ (Dekker and Van Grondelle 2000, Groot et al. 2005, Holzwarth et al. 2006). In this study, the minimal model to describe the recorded fluorescence kinetics takes only two CS phases into account. We will come back to this point later.

To control the model within the limits of data quality, we assumed that the emission spectrum of the relaxed antenna (A) is (more or less) equal to that of the RC (RC). The high spectral overlap of the room temperature emission spectra of CP43, CP47 and RC (Andrizhiyevskaya 2005b) supports the plausibility of this assumption. Spectral constraints are useful in that they facilitate greater insight into the system under study, in particular the rate constants, as the number of free parameters is reduced. Figure 4 displays the SAS resulting from the modeling of Figure 3. The blue antenna (bA) shows an emission maximum at 675 nm, whereas the relaxed antenna (A) and the RC (RC) have their emission peak at 684 nm. RP1 does not fluoresce. The initial excitation ratio between bA, A and RC was estimated to be 40 : 40 : 20. This ratio is in accordance with the near 20% contribution of the RC to the total amount of Chls *a* in the PSII core, and the additional absorption by the two Pheos in the RC at 400 nm. Similarly, from the rate constants in Figure 3, it is observed that the equilibrium between the RC and the antenna is for more than 80% at the side of the antenna ($k_{RC\text{-}A} = 4 \cdot k_{A\text{-}RC}$). The lifetimes determined in the target analysis are 0.5, 1.5, 7.7, 44 and 225 ps. Due to the spectral constraints put in the target analysis it became possible to resolve the extra 1.5 ps decay time with respect to global analysis (Figure 1). Global analysis lacks resolution to discern between decay times of 0.7 and 1.5 ps (Van Stokkum et al. 2004). Note that the other lifetimes are in good accordance with those estimated in the global analysis.

Since each determined fluorescence lifetime is a function of all the decay rates present in the system, each compartment will have some contribution at the different lifetimes. From the target analysis of Figure 3, DAS can be calculated and are shown in Figure 5. The amplitude matrix is presented in Table 1. We will focus

on the main lifetime contributions for each compartment. On the sub-ps time scale, bA, A and RC become populated from the Soret in the ratio 40 : 40 : 20. The lifetime of 1.5 ps is observed (Figure 5) to describe fluorescence decay with emission maximum at 684 nm. From Table 1 it is seen that this lifetime represents trapping of excitation energy from the RC by primary CS, i.e. formation of RP1, upon direct excitation of the RC. From the model in Figure 3, RP1 is observed to form a deep trap, with free energy difference with the RC of -110 meV and a very minor back transfer rate. The DAS of the 7.7 ps lifetime is observed to describe energy transfer from pigments emitting at 670 nm (positive amplitude) to those emitting at 684 nm (negative amplitude) (Figure 5). The amplitude matrix (Table 1) reveals that this transfer belongs to the excitation energy equilibration between bA and A pigments in the CP43/CP47 antenna. It is unclear, why this equilibration time is about twice as large as was estimated earlier (at 77 K) in isolated CP43 and CP47 (De Weerd et al. 2002a). The DAS with 44 ps lifetime and emission maximum at 682 nm (Figure 5) has a significantly larger amplitude and is 2 nm blue-shifted with respect to the 1.5 ps DAS, which is indicative of a role of the antenna in this slow decay phase. From Table 1 it is clearly observed that this lifetime is associated with primary CS and that the energy comes dominantly from bA and A as judged from their significant positive amplitudes at this lifetime. Thus, RP1 formation on the 44 ps time scale arises due to slow energy transfer from the CP43/CP47 antenna to the RC, whereas CS from the directly excited RC occurs on a very fast time scale of 1.5 ps (Table 1). The decay amplitude of the excited RC is small for the 44 ps lifetime (Table 1) because of the inverted kinetics taking place: the excited state of RC becomes populated on a slower time scale (44 ps), then it decays into RP1 (1.5 ps). Finally, RP1 is observed to decay with a 225 ps lifetime (Table 1). If we compare the estimated time scales in this study of RP1 formation (1.5 and 44 ps) and trapping (225 ps) with former studies, RP1 can likely be assigned to a mixture of $Chl_{D1}^{+}Pheo^{-}$ and $P_{680}^{+}Pheo^{-}$ (Groot et al. 2005), whereas the trap will be formed by the $P_{680}^{+}Q_{A}^{-}$ radical pair (Dekker and Van Grondelle 2000).

Important observations from these room temperature data analyses are that 1) the excitation energy equilibration in the CP43/CP47 antenna (bA ↔ A) takes place on a slower time scale (7.7 ps) than assumed in the ERPE model (< 3 ps) (Schatz et al. 1988); 2) this is even more dramatically true for the excitation energy equilibration between the CP43/CP47 antenna and the RC, which is found to occur on a 44 ps time scale and 3) CS from directly excited RC occurs on the very fast time scale of 1.5 ps and is nearly irreversible. We can thus conclude from this

analysis that excitation energy trapping in intact PSII cores with Q_A oxidized can be described well by a model characterized by slow transfer from the antenna to the trap and a fast CS reaction.

Other kinetic models

In order to compare our conclusions with the results of Miloslavina and co-workers (2006) on PSII core kinetics with open RCs, we tried to fit their proposed kinetic model to our data, see Figure 6 and 7 for the model and its SAS, respectively. These authors concluded from their modeling that the energy transfer

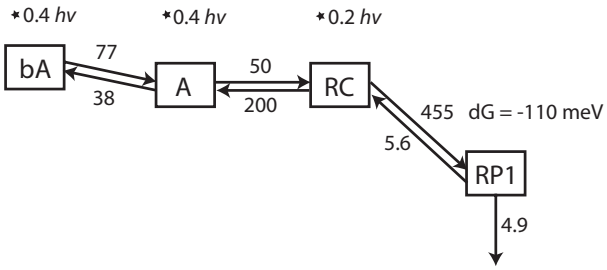

Fig 3. Kinetic model to describe the results of Figure 1. The compartment bA represents the blue absorbing Chls in the CP43/CP47 antenna, which are in equilibrium with the bulk Chls of the antenna (A). The excited RC Chls are represented by (RC), which are in equilibrium with both the core antenna and the first radical pair (RP1). Rate constants (ns^{-1}) resulting from the optimal fit are assigned in the figure as well as the RC-RP1 free energy. Resulting lifetimes: 1.5, 7.7, 44 and 225 ps. The estimated error in the lifetimes is 10%.

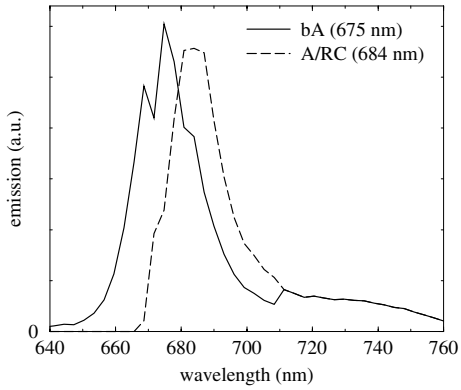

Fig 4. Resulting SAS from the model given in Figure 3. Solid = bA and dashed = A and RC, which have been assumed to have equal spectra. RP1 is non-fluorescent.

between core antenna and RC is much faster than CS, in contrast with our model described above. The quality of the fit of the model of Miloslavina and co-workers (2006) is equal to that of the model displayed in Figure 3 (results not shown), and thus indicates that the model of Figure 3 is not a unique way to describe the data. In this fit (Figure 6), lifetimes of 1.8, 7.5, 46 and 249 ps are estimated, which are highly similar to the values found by Miloslavina and co-workers (2006) (1.5, 7, 10, 42 and 351 ps). We note, however, that Miloslavina and co-workers (2006) required two more components with lifetimes of 111 and 2350 ps running parallel to the model. The 10 ps lifetime, absent in our fit, was assigned to the equilibration between CP43 and CP47 through the RC. Since we do not spectrally discern between the two antenna units, we cannot verify the presence of this component in our data. Table 2 displays the amplitude matrix associated with the model in Figure

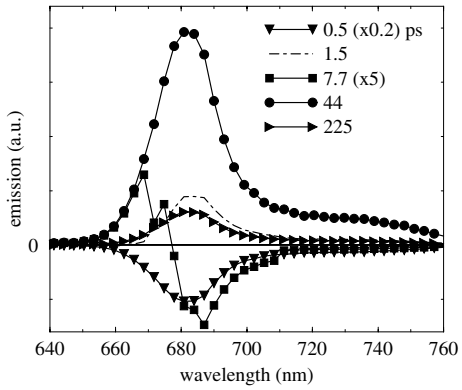

Fig 5. DAS calculated with the help of the kinetic model of Figure 3. See Table 1 for the associated amplitude matrix of the different compartments used in the model.

	bA	**A**	**RC**	**RP1**
τ (ps)	*0.4 hv*	*0.4 hv*	*0.2 hv*	-
1.5	0.006	-0.081	0.182	-0.142
7.7	0.056	-0.071	-0.015	0.026
44	0.304	0.479	0.018	-0.975
225	0.034	0.073	0.015	1.091

Table 1. Amplitude-matrix for the target analysis of the time-resolved fluorescence of intact PSII cores with open RCs at room temperature as presented in Figures 3-5. Negative amplitude represents a population rise, whereas positive amplitude shows population decay of the respective compartment with the specified lifetime.

6, from which it can be seen that energy equilibration between the RC and CP43/CP47 antenna according to this model occurs on the 1.8 ps time scale; RP1 formation takes place with a 7.5 ps time-constant; dominant population decay of the CP43/CP47 antenna, the RC and RP1 occurs on the time scale of 46 ps and finally the energy becomes trapped from RP2 at the time scale of 249 ps. A larger drop in free energy is found for the RP1 to RP2 (60.8 meV) transition, with respect to the primary – RC to RP1 – CS (39.7 meV) (Table 2). All these observations are highly similar to the findings by Miloslavina and co-workers (2006).

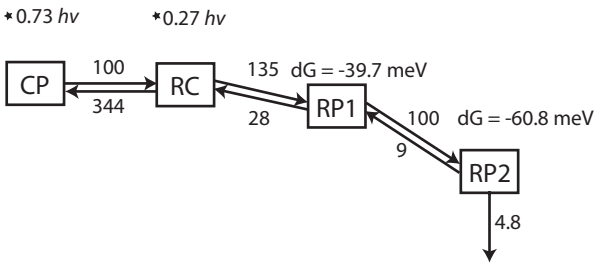

Fig 6. Kinetic model to describe the results of Figure 1, conform (Miloslavina et al. 2006). The compartment CP represents the total core antenna. The excited RC (RC) is in equilibrium with both the core antenna and the first radical pair (RP1). RP1 is in equilibrium with the second radical pair (RP2), which irreversibly traps the excitation energy. Rate constants (ns^{-1}) resulting from the optimal fit are assigned in the figure as well as the RC-RP1 and RP1-RP2 free energy. Resulting lifetimes: 1.8, 7, 46 and 249 ps. The estimated error in the lifetimes is 10%.

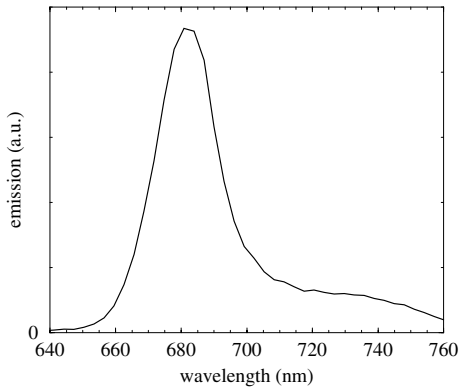

Fig 7. Resulting SAS from the model given in Figure 6, describing the assumed spectral equality of CP43/CP47 antenna and RC with emission maximum at 682 nm. RPs are non-fluorescent.

We conclude that both our model (Figure 3) and that proposed by Miloslavina and co-workers (2006) (Figure 6), describe the actual fluorescence data equally well. In both cases the spectral degeneracy of the CP43, CP47 and RC complexes and their respective pigment contents, causes the excited state equilibrium to be at the side of the antenna. Due to this equilibrium, the *apparent* excited state decay time of the antenna will be longer than the *intrinsic* energy transfer time from the antenna into the RC. Another reason for the deviation between these two time scales is the amount of back transfer occurring from the RPs to the RC excited state, as well as the rate of CS. These rates cause the excitations to travel back and forth between the RPs and the antenna, resulting in an increased time spent in the antenna, due to the A-RC equilibrium. In Miloslavina's model, RP1 formation occurs on a time scale of 7.5 ps and the back transfer into the RC is rather significant. The *intrinsic* energy transfer time scale from the antenna to the RC is 10 ps (Figure 6). In our model, however, RP1 forms a deep trap (1.5 ps) from which back transfer occurs to a much lesser extent (Figure 3) than in the model of Miloslavina (Figure 6). The *intrinsic* energy transfer time from the antenna to the RC is 20 ps (Figure 3). Consequently, in our model, the direct antenna to RC energy transfer plays a more significant role in the *apparent* excited state decay time of the antenna than is the case in Miloslavina's model, which is ~45 ps in both cases. The inverted kinetics mentioned earlier for the RC in the model of Figure 3 (Table 1) confirms this conclusion and suggests a non-negligible role for antenna to RC energy transfer in the total CS process.

From the X-ray structure of PSII cores, inter-pigment distances between CP43/CP47 and the RC appeared to be rather large with respect to the distances between the pigments in a single complex. This raised the question whether energy equilibration between the antenna and the RC could occur as fast as proposed by

	CP	**RC**	**RP1**	**RP2**
τ (ps)	*0.73hv*	*0.27 hv*	-	-
1.8	-0.08	0.10	-0.03	0.006
7.5	0.04	-0.004	-0.17	0.164
46	0.68	0.15	0.1	-1.17
249	0.09	0.024	0.1	1.00

Table 2. Amplitude-matrix for the target analysis of the time-resolved fluorescence of intact PSII cores with open RCs at room temperature as represented in Figures 6,7. Negative amplitude represents a population rise, whereas positive amplitude shows population decay of the respective compartment with the specified lifetime.

the ERPE model (< 3 ps). The model according to Miloslavina and co-workers (2006) in Figure 6, shows forward and backward rates of respectively 100 and 344 ns^{-1} between the antenna and the RC. From our proposed model in Figure 3 we observe both rates to be smaller, that is, 50 and 200 ns^{-1} respectively. Consequently, the *intrinsic* energy equilibration time between the antenna and the RC will be larger in our modeling (Figure 3) than is the case in Miloslavina's model (Figure 6). Moreover, within our proposed model we were able to resolve the spectral evolution between the blue and 'red' antenna pigment pools of CP43/CP47 (bA and A), with an *apparent* equilibration time of 7.5 ps. Referring to the X-ray structure, the equilibration between the CP43/CP47 antenna and the RC will take place on a much larger time scale than equilibration within the CP43/CP47 antenna. Indeed, the *apparent* equilibration time between antenna and RC is observed to be 44 ps from Table 1. Both equilibration times within the antenna and between the antenna and the RC are thus significantly larger than the proposed < 3 ps equilibration time by the ERPE model. However, from Table 2 it is observed that Miloslavina's model results in an *apparent* energy equilibration time between antenna and RC of only 1.5 ps. Consequently, the model in Figure 3 is favored with respect to that proposed by Miloslavina and co-workers (2006), since it is fully consistent with the predictions from the X-ray structure.

The spectral degeneracy of the CP43 and CP47 antenna units with the RC, causes time-resolved visible absorption and emission spectroscopy to be incapable to distinguish between the pigments of either complex. To this end, time-resolved infrared spectroscopy is required, since each complex has a specific infrared fingerprint. More importantly, Chl and Pheo have unique signatures in their different charged states (Groot et al. 2005). Thus, infrared spectroscopy could reveal the role of CS in the recorded slow decay phases. However, this type of experiment is not possible with low excitation light intensities, which are required to keep the RCs of PSII core open. Time-resolved infrared measurements have been performed on isolated RCs (Groot et al. 2005) and revealed the identity of the primary electron donor-acceptor pair ($Chl_{D1}^{+}Pheo^{-}$) as well as the ultrafast time scale on which it is formed, 0.6-0.8 ps. This ultrafast time scale of primary CS, is in support of our modeling of the PSII core kinetics according to Figure 3, which resulted in 1.5 ps for RP1 formation, over that proposed by Miloslavina and co-workers (2006) where 7.5 ps was found (Figure 6). Recently, Pawlowicz and co-workers (2007) have measured the mid-infrared kinetics of PSII cores at room temperature. The data could be well fit using the same kinetic model for the PSII core RC as was found for the isolated RC (Groot et al. 2005) and adding two

slowly transferring antennae. From the target analysis, fast CS is found to occur in the PSII core on a time scale of 3 ps. The charge separated state is identified as $P_{680}^{+}Pheo^{-}$. The $Chl_{D1}^{+}Pheo^{-}$ state is not observed and therefore concluded to have a very minor population. Consequently, $Chl_{D1}^{+}Pheo^{-}$ is assumed to be mixed with the excited RC in the applied model. $P_{680}^{+}Pheo^{-}$ formation is determined to occur on a second time scale of 27 ps as well. The slow $P_{680}^{+}Pheo^{-}$ formation is clearly shown to be due to the slow energy equilibration between the CP43/CP47 antenna and the RC, with 40 ps *intrinsic* energy transfer time-constant from the antenna to the RC. Note how the results presented in this paper (Figure 3, Table 1) agree with the biphasic RP1 formation and the slow energy transfer from the antenna to the RC found in the mid-infrared study of PSII cores (Pawlowicz et al. 2007). In contrast, Miloslavina and co-workers (2006) assigned the 42 ps lifetime to slow radical pair formation.

Finally, note that the free energy difference associated with RP1 formation in the model of Figure 3 is -110 meV, or 890 cm^{-1}, which is in full agreement with the simulations of (Broess et al. 2006), modeling two RPs, from which it was concluded that primary CS in open RCs of PSII membranes must be fast and nearly irreversible.

77 K time-resolved emission

To support the conclusions drawn from the room temperature measurements, that is, to show that the energy transfer from the antenna to the RC is slow, time-resolved emission was recorded of PSII cores at 77 K. Note that at this temperature and given the experimental conditions, it was not possible to keep the RCs open, but this is of no influence in estimating the excitation energy migration time. Although cryogenic temperatures promote selective excitation, to avoid artifacts introduced by the large contribution of Rayleigh scattering in this type of experiment, the time-resolved emission of PSII cores was recorded at 77 K upon 400 nm excitation.

The resulting DAS from global analysis are shown in Figure 8. An overall negative spectrum with maximum at 682 nm and a lifetime of 3.3 ps describes the Soret relaxation (note that the FWHM of the overall time response is 10 ps). At the 7.4 ps time scale energy transfer is clearly observed to occur from pigments emitting at 675 nm (positive amplitude) to those with emission wavelength at 685.5 nm (negative amplitude). Note, that since a significant rise of fluorescence is recorded (negative amplitude), CS in the RC can thus not be the main process occurring at this time scale. The main decay component has a lifetime of 29 ps, and

its emission maximum is at 682.5 nm. At the same time scale, the small negative amplitude at long wavelengths indicates that a small amount of energy is transferred to pigments with emission maximum at 693 nm. A Chl *a* with this red emission wavelength is known to be located in CP47 (Den Hartog et al. 1998, De Weerd et al. 2002b, Groot et al. 2004). As a result, the 29 ps time-constant will include the migration time of excitations in the CP47 antenna to the 693 nm trap. A decay phase with time-constant of 169 ps is observed with maximum emission at 684 nm (Figure 8). In an earlier study (Van der Weij – de Wit et al. 2007) the main trapping phase in PSII membranes (BBY) and in intact photosynthetic membranes at 77 K was shown to have a similar lifetime of 150 ps. In BBY this spectrum is somewhat broader and the emission maximum is 3 nm blue-shifted (Van der Weij – de Wit et al. 2007), due to the binding of light-harvesting complex II, which causes the excitation distribution to be blue-shifted. On the ns time scale two more fluorescence decay phases are resolved with respective lifetimes of 1 and 6 ns (Figure 8). The 1 ns decay component has an emission maximum at 688 nm, whereas the 6 ns component displays two peaks respectively at 687 and 695 nm, recognized as the PSII core steady-state emission spectrum at 77 K (Andrizhiyevskaya et al. 2005a). In BBY (Van der Weij – de Wit et al. 2006) a phase with 500 ps decay time resembles the 1 ns phase resolved in cores (Figure 8). In the following we will argue that this phase corresponds to the formation of a third radical pair. Therefore, the difference in this lifetime between cores and BBY will be due to the role of the antenna in determining the RP relaxation mechanism. Similarly, in BBY (Van der Weij – de Wit et al. 2007) a phase with 4 ns lifetime and emission maximum at 693 nm was determined to represent trapping on the red

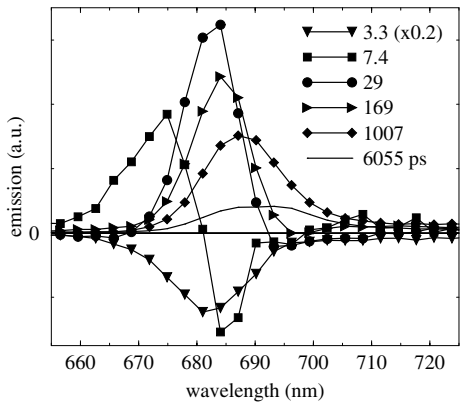

Fig 8. DAS of intact PSII cores at 77 K upon 400 nm excitation.

pigments of CP47. In the core (Figure 8) the 6 ns spectrum has a clear contribution at 687 nm as well. We conclude the presence of a small fraction of free CP43/CP47 antenna units due to the freezing and thawing of the PSII core sample.

Kinetic modeling

A target analysis was performed to identify the individual processes contributing to the DAS of Figure 8. The minimal model comprises six compartments, see Figure 9, which includes the optimal rate constants and the RP free energies. The compartments respectively represent bulk antenna (bA), non-equilibrated antenna (A), equilibrated antenna and RC (RC), RP1, RP2 and red pigments of CP47 (A_{red}). In this analysis the RC compartment is thus considered to be the RC in equilibrium with the CP43/CP47 antenna, since the S/N ratio of the data did not allow the determination of more equilibria than the ones shown in Figure 9, which are necessary to describe the charge-recombination. Similarly, the bulk (bA) to non-equilibrated antenna (A) energy transfer depicted in Figure 9 represents the blue to red Chl *a* energy relaxation taking place in the CP43 and CP47 antenna. The initial excitation population was chosen to be 80 : 0 : 20 between bulk antenna (bA), non-equilibrated antenna (A) and the antenna in equilibrium with the RC (RC), thus considering the blue to red Chl *a* energy relaxation in the CP43/CP47 antenna irreversible. This assumption is reasonable, since back transfer to blue antenna pigments will be significantly smaller at this temperature than at room temperature (Figure 3). Notice that we use a somewhat different approach to describe the 77 K data than those collected at room temperature (Figure 3). At 77 K the spectral resolution is much better due to the strong reduction of homogeneous broadening, though the S/N of the data is still insufficient to spectrally distinguish between CP43 and CP47. But we do, however, distinguish between internal antenna diffusion (bA → A) and transfer to the trap (A → RC), which is the purpose of this experiment. The 77 K SAS resulting from the modeling in Figure 9 are displayed in Figure 10 and show overlap between bulk (bA) and non-equilibrated antenna (A), where the bulk antenna has extra emission amplitude at blue wavelengths due to which it has an emission maximum at 683 nm and the non-equilibrated antenna at 684 nm. The antenna in equilibrium with the RC (RC) shows its emission maximum at 685.5 nm. The red pigments of CP47 show an emission maximum at 693 nm. RP1 and RP2 are non-fluorescent. The calculated DAS and amplitude matrix of the model in Figure 9 are respectively shown in Figure 11 and Table 3. The fluorescence rise as a result of Soret to Q_Y relaxation is fixed to take place on the sub-picosecond time scale. The 3.3 ps

lifetime DAS shows overall positive amplitude (Figure 11) with emission maximum at 685.5 nm. Primary CS is seen to dominate the 3.3 ps lifetime (Table 3), which is thus a factor two slower than for PSII cores with open RCs at room temperature (Table 1). This result is in good accordance with the estimated 1-4 ps time scale of RP1 formation in the isolated RC at 77 K (Visser et al. 1995, Konermann et al. 1997, Groot et al. 1997). On the 7 ps time scale, energy transfer is obviously taking place from Chls with emission maximum at 674 nm to those with emission at 685 nm (Figure 11). From the amplitude matrix (Table 3) the transfer is concluded to be due to blue to red Chl *a* excitation energy relaxation (bA

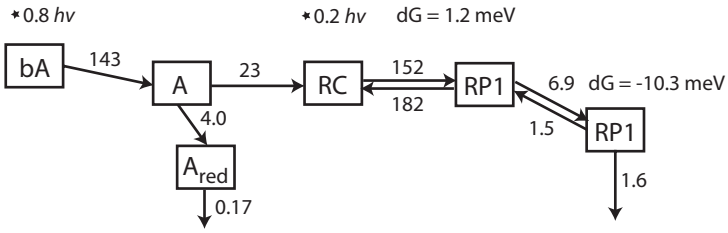

Fig 9. Kinetic model to describe the results of Figure 8. The compartment bA represents the blue absorbing Chls in the CP43/CP47 antenna, which relax to the non-equilibrated bulk Chls of the antenna (A). The compartment (RC) represents the equilibrium between core antenna and excited RC. Note that this is different than for the room temperature kinetic model of Figure 3. Two RPs (RP1, RP2) are in equilibrium with the RC and its associated core antenna. Rate constants (ns^{-1}) resulting from the optimal fit are assigned in the figure as well as the free energies. Resulting lifetimes: 0.5, 3.3, 7, 37, 193, 1046 and 5000 ps. The estimated error in the lifetimes is 10%.

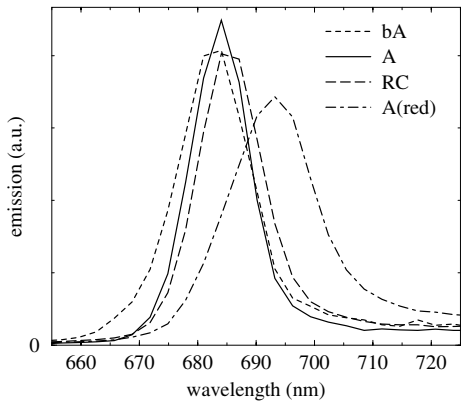

Fig 10. Resulting SAS from the model given in Figure 9.

→ A) in the antenna, see also Figure 8. The lifetime and interpretation of this phase is almost identical to that of the corresponding phase with similar kinetics at room temperature. The 37 ps lifetime has a main positive contribution from non-equilibrated antenna (Table 3) and negative amplitude by RP1. Thus, RP1 formation is biphasic, with time scales of 3.3 and 37 ps, the latter being due to slow transfer from the antenna. This result is similar to that at room temperature, where direct CS from the RC occurs on the 1.5 ps time scale and slow transfer from the antenna resulted in a second formation time of 44 ps (Table 1). From the negative amplitude in Table 3, as well as that at 693 nm in Figure 11, it is concluded that also the red pigments of CP47 become populated at the time scale of 37 ps. Note

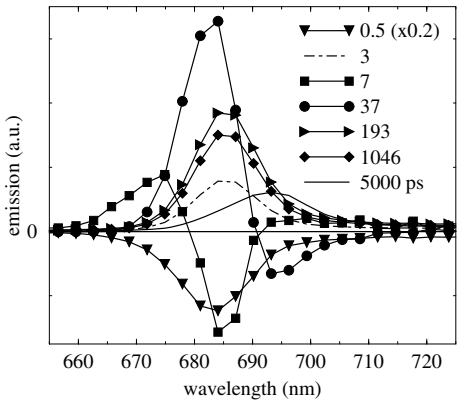

Fig 11. DAS calculated with the help of the kinetic model of Figure 9. See Table 3 for the associated amplitude matrix of the different compartments used in the model.

	bA	**A**	**RC**	**RP1**	**RP2**	**A_{red}**
τ (ps)	*0.8 hv*	-	*0.2 hv*	-	-	-
3.0	-	-	0.130	-0.133	0.003	-
7.0	0.8	-1.0	0.042	0.138	-0.007	0.030
37	-	1.0	-0.517	-0.461	0.135	-0.149
193	-	-	0.300	0.249	-0.798	-
1046	-	-	0.245	0.207	0.667	-
6024	-	-	-	-	-	0.119

Table 3. Amplitude-matrix for the target analysis of the time-resolved fluorescence of intact PSII cores at 77 K as represented in Figures 8-11. Negative amplitude represents a population rise, whereas positive amplitude shows population decay of the respective compartment with the specified lifetime.

how this migration time scale in the CP47 antenna (37 ps) resembles that in the trimeric LHCII complex, which was estimated to be ~32 ps (Barzda et al. 2001) and how this time scale is slower than measured before in isolated CP47 at 77 K (de Weerd et al. 2002a). From Table 3, both (RC) and (RP1) populations are observed to decay, whereas RP2 is seen to be formed on the 193 ps time scale. RP2 trapping is observed to give rise to the dominant fluorescence decay component (Figure 8,11), which is expressed by the -10 meV RP1-RP2 free energy difference with respect to the shallow RC-RP1 trap (1.2 meV) (Figure 9). The 1 ns lifetime displays positive amplitudes from RC, RP1 and dominantly RP2 (Table 3), since it is the decay time of RP2 into the final RP trap state. Then, the excitations which were trapped on the red pigments of CP47 are seen to decay on the 6 ns time scale (Figure 11, Table 3), which agrees well with the 5.8 ps fluorescence lifetime of CP47 at 77 K as estimated by De Weerd and co-workers (2002a).

At 77 K, the CS in the PSII core will be different from that at room temperature, since Q_A is in its reduced form at this temperature. RP1, formed on the 3.3. ps time scale, is assigned to $Chl_{D1}^{+}Pheo^{-}$ (Groot et al. 2005). Electron transfer from RP1 to RP2 occurs on the time scale of 193 ps and RP2 is assigned to $P^{+}Pheo^{-}$. The final RP trap in PSII cores with Q_A reduced is likely a relaxed state of $P^{+}Pheo^{-}$ (Konermann et al. 1997). Note that RP1 is nearly iso-energetic with the excited RC (1.2 meV) (Figure 9) and thus forms an extremely shallow trap, causing the excitations to travel back and forth between the antenna, RC and RP1 many times before trapping occurs. Consequently, the (RC) compartment, representing the RC in equilibrium with the CP43/CP47 antenna, shows large decay amplitudes at long time scales of 193 ps and 1 ns in the amplitude matrix of Table 3. The same is true for the decay amplitudes of RP1 (Table 3). At 77 K the excited state decay in the PSII core will thus be trap-limited. From Table 3, the energy transfer from the CP43/CP47 antenna into the RC is observed to take place on the time scale of 37 ps at 77 K.

Concluding, the 77 K experiment shows that excitation energy relaxation within the CP43 or CP47 antenna takes place at a time scale of 7 ps, which is similar to the value found at room temperature (7.7 ps). The excitation energy transfer from CP43 or CP47 to the RC was determined to occur on a 37 ps time scale at 77 K (Figure 9, Table 3), similar to the value found at room temperature (44 ps, Figure 3, Table 1). Note from Figure 9 that the excited state of the non-equilibrated antenna (A) does not become populated through back transfer from the RPs and as such represents the true energy transfer time among the antenna and RC. It is concluded that energy transfer from the antenna into the RC is slow in

PSII cores. RP1 formation from the excited RC, however, occurs on a faster time scale at room temperature (1.5 ps) than at 77 K (3.3 ps). The latter is explained by the different RP relaxation mechanisms in the presence of oxidized Q_A at room temperature and reduced Q_A at 77 K (Konermann et al. 1997, Andrizhiyevskaya 2005b).

Conclusions

We have performed time-resolved fluorescence measurements of PSII cores with open, functional RCs at room temperature. By kinetic modeling, charge separation was found to occur at an ultrafast time scale of 1.5 ps, consistent with recently estimated ultrafast RP1 formation by femtosecond infrared spectroscopy (Groot et al. 2005). RP1 formation was found to be virtually irreversible in this study, which is in accordance with modeling performed on time-resolved fluorescence data of PSII membranes with open RCs (Broess et al. 2006). Energy equilibration within the antenna was found to take place at a time scale of 7.7 ps. Energy equilibration between the antenna and the RC was estimated to take place at a 44 ps time scale (Table 1). Slow energy transfer from the antenna to the RC occurring with an estimated *intrinsic* time scale of 20 ps (Figure 3), plays a significant role in this equilibration time. Excitation energy equilibration between antenna and RC is thus found to occur on a larger time scale than proposed by the ERPE model (< 3 ps) and consequently meets predictions from the X-ray structure (Dekker and Van Grondelle 2000, Vasil'ev et al. 2001, Broess et al. 2006).

At 77 K, time-resolved fluorescence measurements of PSII cores revealed the energy equilibration time in the core antenna to be of similar size (7 ps) as was estimated at room temperature. The same is true for the excited state decay of the antenna, which was determined to occur at the time scale of 37 ps at 77 K. We conclude that population of the RC from the CP43/CP47 antenna takes place at a much longer time scale (> 10x) than primary CS, both at room temperature and at 77 K. Consequently, the time scale of energy transfer from the CP43/CP47 antenna into the RC can not be neglected in the total CS kinetics in intact cores, due to which CS will not be purely trap-limited.

Acknowledgments

This work is part of the research programme of the 'Stichting voor Fundamenteel Onderzoek der Materie (FOM)', which is financially supported by the

‘Nederlandse Organisatie voor Wetenschappelijk Onderzoek (NWO)’.

Literature

Andrizhiyevskaya, E.G., Chojnicka, A, Bautista, J.A., Diner, B.A., Van Grondelle, R., Dekker, J.P. (2005a) Origin of the F685 and F695 fluorescence in Photosystem II, Photosynth. Res. 84, 173-180.

Barzda, V., Gulbinas, V., Kananavicius, R., Van Amerongen, H., Van Grondelle, R., Valkunas, L. (2001) Singlet-singlet annihilation kinetics in aggregates and trimers of LHCII. Biophys. J. 80, 2409-2421.

Broess, K., Trinkunas, G., Van der Weij – de Wit, C.D., Dekker, J.P., Van Hoek, A., Van Amerongen, H. (2006) Excitation energy transfer and charge separation in photosystem II membranes revisited, Biophys. J. 91, 3776-3786.

Dekker, J.P. and Boekema, E.J. (2005) Supramolecular organization of the thylakoid membrane proteins in green plants, Biochim. Biophys. Acta 1706, 12-39.

Dekker, J.P. and Van Grondelle, R. (2000) Primary charge separation in photosystem II, Photosynth. Res. 63, 195-208.

De Weerd, F.L., Van Stokkum, I.H.M., Van Amerongen, H., Dekker, J.P., Van Grondelle, R. (2002a) Pathways for energy transfer in the core light-harvesting complexes CP43 and CP47, Biophys. J. 82, 1586-1597.

De Weerd, F.L., Palacios, M.A., Andrizhiyevskaya, E.G., Dekker, J.P., Van Grondeller, R. (2002b) Identifying the lowest electronic states of the chlorophylls in the CP47 core antenna protein of photosystem II, Biochemistry 41, 15224-15233.

Den Hartog, F.T.H., Dekker, J.P., Van Grondelle, R., Völker, S. (1998) Spectral distributions of “trap” pigments in the RC, CP47, and CP47-RC complexes of photosystem II at low temperature: a fluorescence line-narrowing and hole-burning study, J. Phys. Chem. B, 11007-11016.

Diner, B.A. and Rappaport, F. (2002) Structure, dynamics, and energetics of the primary photochemistry of photosystem II of oxygenic photosynthesis, Annu. Rev. Plant Biol. 53, 551-580.

Ferreira, K.N., Iverson, T.M., Maghlaoui, K., Barber, J., Iwata, S. (2004) Architecture of the photosynthetic oxygen-evolving center, Science 303, 1831-1838.

Groot, M.L., Van Mourik, F., Eijckelhoff, C., Van Stokkum, I.H.M., Dekker, J.P.,

Van Grondelle, R. (1997) Charge separation in the reaction center of photosystem II studied as a function of temperature, Proc. Natl. Acad. Sci. 94, 4389-4394.

Groot, M.L., Breton, J., Van Wilderen, L.J.G.W., Dekker, J.P., Van Grondelle, R. (2004) Femtosecond visible/visible and visible/mid-ir pump-probe study of the photosystem II core antenna complex CP47, J. Phys. Chem. B 108, 8001-8006.

Groot, M.L., Pawlowicz, N.P., Van Wilderen, L.J.G.W., Breton, J., Van Stokkum, I.H.M., Van Grondelle, R. (2005) Initial electron donor and acceptor in isolated photosystem II reaction centers identified with femtosecond mid-IR spectroscopy, Proc. Natl. Acad. Sci. 102 (37), 13087-13092.

Holzwarth, A.R. (1996) Data analysis of time-resolved measurements, In: Amesz, J. and Hoff, A.J. (eds) Biophysical Techniques in Photosynthesis, 75-92. Kluwer Academic Publishers, Amsterdam.

Holzwarth, A.R., Müller, M.G., Reus, M., Nowaczyk, M., Sander, J., Rögner, M. (2006) Kinetics and mechanism of electron transfer in intact photosystem II and in the isolated reaction center: pheophytin is the primary electron acceptor, Proc. Natl. Acad. Sci. 103 (18), 6895-6900.

Kern, J., Loll, B., Laaneberg, C., DiFiore, D., Biesiadka, J., Irrgang, K.-D., Zouni, A. (2005) Purification, characterisation and crystallisation of photosystem II from Thermosynechococcus elongates cultivated in a new type of photobioreactor, Biochim. Biophys. Acta 1706, 147-157.

Konermann, L., Gatzen, G., Holzwarth, A.R. (1997) Primary processes and structure of the photosystem II reaction center. 5. Modeling of the fluorescence kinetics of the D1-D2-cyt-b559 complex at 77 K, J. Phys. Chem. B 101, 2933-2944.

Loll, B., et al. (2005) Towards complete cofactor arrangement in the 3.0 angström resolution structure of photosystem II, Nature 438 (7070), 1040-1044.

Miloslavina, Y., Szczepaniak, M., Müller, M.G., Sander, J., Nowaczyk, M., Rögner, M., Holzwarth, A.R. (2006) Charge separation kinetics in intact photosystem II core particles is trap-limited. A picosecond fluorescence study, Biochem. 45, 2436-2442.

Nelson, N. and Yocum, C.F. (2006) Structure and function of photosystem I and II, Annu. Rev. Plant. Biol. 57, 521-565.

Pawlowicz, N.P., Groot, M.L., Van Stokkum, I.H.M., Breton, J., Van Grondelle, R. (2007) Charge separation and energy transfer in the photosystem II core complex studied by femtosecond mid-infrared spectroscopy, submitted.

Schatz, G.H., Brock, H., Holzwarth, A.R. (1987) Picosecond kinetics of fluorescence and absorbance changes in photosystem II particles excited at low photon density, Proc. Natl. Acad. Sci. 84, 8414-8418.

Schatz, G.H., Brock, H., Holzwarth, A.R. (1988) A kinetic and energetic model for the primary processes in photosystem II, Biophys. J. 54, 397-405.

Van Grondelle, R., Dekker, J.P., Gillbro, T., Sundström (1994) Energy transfer and trapping in photosynthesis, Biochim. Biophys. Acta 1187, 1-65.

Van Grondelle, R. (1985) Excitation energy transfer, trapping and annihilation in photosynthetic systems, Biochim. Biophys. Acta 811, 147-195.

Van Mieghem, F.J.E., Searle, G.F.W., Rutherford, A.W., Schaafsma, T.J. (1992) The influence of the double reduction of QA on the fluorescence decay kinetics of photosystem II, Biochim. Biophys. Acta 1100, 198-206.

Van der Weij – de Wit, C.D., Ihalainen, J.A., Van Grondelle, R., Dekker, J.P. (2007) Excitation energy transfer in native and unstacked thylakoid membranes studied by low temperature and ultrafast fluorescence spectroscopy, Photosynth. Res., submitted.

Van Stokkum, I.H.M., Larsen, D.S., Van Grondelle, R. (2004) Global and target analysis of time-resolved spectra, Biochim Biophys Acta 1657, 82-104.

Vasil'ev, S., Orth, P., Zouni, A., Owens, T.G., Bruce, D. (2001) Excited-state dynamics in photosystem II: insights from the x-ray crystal structure, Proc. Natl. Acad. Sci. 98 (15), 8602-8607.

Vasil'ev, S., Lee, C.-I., Brudvig, G.W., Bruce, D. (2002) Structure-based kinetic modeling of excited-state transfer and trapping in histidine-tagged photosystem II core complexes from Synechocystis, Biochem. 41, 12236-12243.

Visser, H.M., Groot, M.L., Van Mourik, F., Van Stokkum, I.H.M., Dekker, J.P., Van Grondelle, R. (1995) Subpicosecond transient absorption difference spectroscopy on the reaction center of photosystem II radical pair formation at 77 K, J. Phys. Chem. 99 (41), 15304-15309.

Zouni, A., Witt, H.-T., Kern, J., Fromme, P., Krauß, N., Saenger, W., Orth, P. (2001) Crystal structure of photosystem II from Synechococcus elongatus at 3.8 Å resolution, Nature 409 (8), 739-743.